ARTICLE Communicated by Christof Koch

Stimulus-Dependent Synchronization of Neuronal Assemblies

E. R. Grannan*
D. Kleinfeld
AT&T Bell Laboratories, Murray Hill, NJ 07974 USA

H. Sompolinsky
Racah Institute of Physics and the Center for Neural Computation, Hebrew University, Jerusalem, 91904 Israel, and AT&T Bell Laboratories, Murray Hill, NJ 07974 USA

We study theoretically how an interaction between assemblies of neuronal oscillators can be modulated by the pattern of external stimuli. It is shown that spatial variations in the stimuli can control the magnitude and phase of the synchronization between the output of neurons with different receptive fields. This modulation emerges from cooperative dynamics in the network, without the need for specialized, activity-dependent synapses. Our results further suggest that the modulation of neuronal interactions by extended features of a stimulus may give rise to complex spatiotemporal fluctuations in the phases of neuronal oscillations.

1 Introduction

A ubiquitous feature of the brain is the presence of widespread, rhythmic patterns of neuronal activity (Ketchum and Haberly 1991). One aspect of this activity is gamma oscillations in the visual cortex, with a frequency near 40 Hz, that are evoked by an external stimulus (Bouyer *et al.* 1981; Freeman and van Dijk 1987; articles in Schuster 1991). Singer and Gray and co-workers (Gray *et al.* 1989; Engel *et al.* 1991a,b) and Eckhorn *et al.* (1988) showed that the timing of these oscillations in a region of cortex can, under certain circumstances, be influenced by visual stimuli that lie outside its receptive field. In particular, the oscillations in regions with nonoverlapping receptive fields are synchronized when the direction of motion and orientation of stimuli presented to the individual fields are similar. Conversely, dissimilarity in these features results in a failure to synchronize. These results suggest that temporal coherence may be used to encode features of objects in multiple receptive fields.

*Present address: Department of Physics, Physical Sciences 2, University of California, Irvine, CA 92717.

Temporal synchrony across the visual cortex (Engel *et al.* 1991a) is most likely mediated by long-range axonal projections within the cortex. These long-range axonal projections appear to connect neurons with different receptive fields but similar orientation preference (Gilbert and Wiesel 1989). However, the mechanism by which the stimulus gates the influence of the long-range connections, and thereby modulates the synchrony of the oscillations, is unclear.

Here we consider theoretically how spatial variations in an extended stimulus can modulate the interactions in a network of coupled neuronal assemblies. Each assembly consists of analog neurons that are extensively interconnected and produce oscillatory output as a result of inhibitory feedback. Neurons in different assemblies are coupled by relatively weak, feature-specific excitatory connections. The strength of all connections are fixed.

Our work was motivated by the results of computer simulations (Sporns *et al.* 1989; Schillen and Konig 1991; Konig and Schillen 1991; Wilson and Bower 1991) and analytical studies (Schuster and Wagner 1991a,b; see also Aertsen *et al.* 1989) that suggest that the magnitude and possibly the phase of the interaction between assemblies can be modulated by the stimulus. Other studies, however, suggested that these effects are insufficiently strong (Sporns *et al.* 1991). Stimulus-dependent synchronizing interactions were postulated ad hoc in a previous theoretical study of a network of phase oscillators (Sompolinsky *et al.* 1990, 1991). It was shown that the emergent synchronization in the network was modulated by the extended properties of the stimulus in a manner similar to that found in experiments. In the present study we derive the form of the synchronizing interactions between the assemblies, and their dependence on spatial variations in the stimulus, from the full dynamics of the network.

2 Model

Our model describes the cooperative behavior of a network of weakly coupled clusters of neurons. Each cluster is analogous to a hypercolumn in primary visual cortex (e.g., Douglas and Martin 1990). It consists of neurons that respond to the presence of a stimulus within its receptive field. For simplicity, we limit ourselves to neurons whose response depends only on a single feature of the stimulus, namely the orientation of an edge. The time averaged value of this response has a pronounced peak at a particular orientation, referred to as the preferred orientation of the neuron. We assume that the preferred orientations are uniformly distributed among different neurons within each cluster. Each cluster contains two types of neurons. One, the excitatory cells, makes only excitatory connections on its postsynaptic target while the second, inhibitory cells, make only inhibitory connections. In our architecture, all

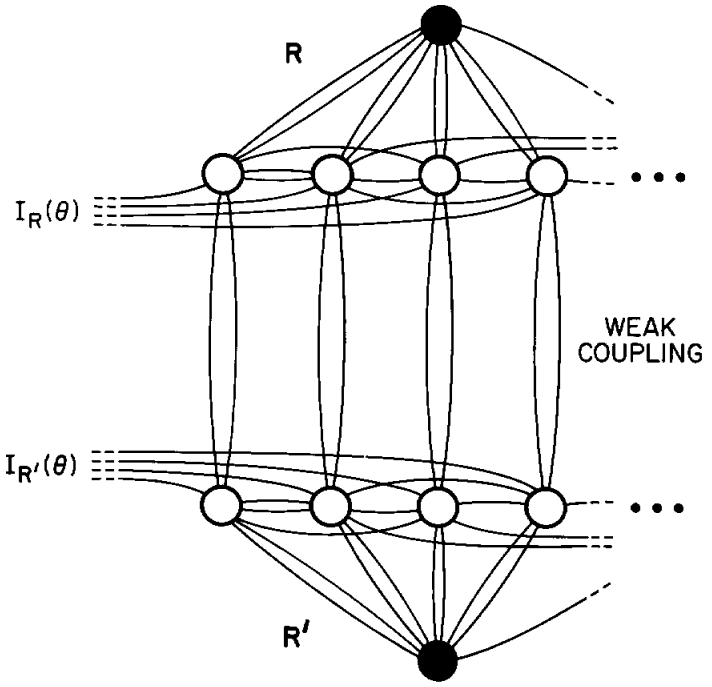

Figure 1: Schematic of the architecture of a network with two clusters. The open circles represent neurons that form only excitatory connections and filled circles represent neurons that make solely inhibitory connections. Only a representative fraction of the total number of connections is drawn.

of the inhibitory neurons are equivalent and can be replaced by a "global" inhibitory cell. There are extensive connections between neurons in the same cluster but only sparse connections between neurons in different clusters. The architecture of a network with two clusters is shown in Figure 1.

The dynamics of the network is described by circuit equations (Wilson and Cowan 1972; Amari 1972; Hopfield 1984):

$$\begin{aligned} \dot{v}_R(\theta,t) &= -v_R(\theta,t) + \frac{J_E}{N}\sum_{\theta'\neq\theta} V_R(\theta',t) + J_I U_R(t) + I_R(\theta) + \xi_R(t) \\ &\quad + \varepsilon \sum_{R'\neq R} K(R-R')V_{R'}(\theta,t) \\ \dot{u}_R(t) &= -u_R(t) + \frac{J'_E}{N}\sum_{\theta'} V_R(\theta',t) \end{aligned} \tag{2.1}$$

where $v_R(\theta, t)$ and $V_R(\theta, t)$ are the potential and output, respectively, of the excitatory neuron with orientation preference θ in the Rth cluster, N is the number of excitatory neurons in a cluster, $u_R(t)$ and $U_R(t)$ are the potential and output of the inhibitory neuron, and time, t, is normalized by the neuronal time constant. The output of each neuron may be interpreted as its instantaneous rate of firing. It depends on the value of the potential through a nondecreasing function, which we assume is the same for all neurons:

$$V_R(\theta, t) = g[v_R(\theta, t)] \qquad \text{and} \qquad U_R(t) = g[u_R(t)] \tag{2.2}$$

The form of $g(x)$ is taken to be the logistic function $g(x) = 1/\{1 + \exp[-4\beta(x - x_0)]\}$, where β and x_0 correspond to the gain and threshold parameters of the neurons, respectively.

The parameters J_E and J_I denote the strength of the synapses from excitatory and inhibitory presynaptic neurons, respectively, to excitatory postsynaptic neurons within the same cluster. The parameter J'_E denotes the strength of the synapses from excitatory neurons to the inhibitory one. We have assumed that these parameters do not depend on the orientation preference of the the pre- and postsynaptic neuron. On the other hand, synapses between the excitatory neurons of two different clusters occur only between neurons with similar orientation preference. These synapses have strength ϵ and their spatial dependence is specified by the function $K(R - R') = K(|R - R'|)$.

The external input consists of two components. A time-independent part, $I_R(\theta)$, encodes the orientation of a single edge within the receptive field of the Rth cluster. It is of the form

$$I_R(\theta) = I(|\theta - \theta_0(R)|) \tag{2.3}$$

where $\theta_0(R)$ denotes the orientation of the stimulus and both θ and θ_0 lie between 0 and π. For simplicity, only the excitatory neurons are taken to have external input. Temporal fluctuations in the input are denoted by a noise term, $\xi_R(t)$. We have assumed that the noise is uniform within each cluster but varies between clusters (Sompolinsky *et al.* 1991). This noise competes with the interactions between different clusters and tends to destroy their relative synchrony. It is taken to be a gaussian variable with zero mean and variance

$$\langle \xi_R(t) \xi_{R'}(t') \rangle = 2\varepsilon T \, \delta_{RR'} \, \delta(t - t') \tag{2.4}$$

where T is the strength of the noise relative to that of the intercluster connections.

A basic assumption in our model is that the neurons within a cluster interact strongly among each other while the interaction between neurons in different clusters is weak. This implies that the value of ε is small compared to that of J_E, J'_E, and $-J_I$. For this condition, we expect that the activity of a neuron is determined primarily by its connections to

neurons in the same cluster and by the stimulus within its receptive field. The dominant effect of the connections between clusters is to modulate the synchrony, that is, the relative phase, between neuronal activities in separate clusters.

In our analysis of the model, we consider first the dynamics of a single cluster and ignore the interactions between clusters as well as the noise. We then derive the effective interaction between pairs of clusters, including the effects of noise, that results from their long-range connections.

3 Single Cluster Dynamics

The equations that describe a single cluster are (the label R is suppressed)

$$\begin{aligned} \dot{v}(\theta,t) &= -v(\theta,t) + J_E V(t) + J_I U(t) + I(\theta) \\ \dot{u}(t) &= -u(t) + J'_E V(t) \end{aligned} \tag{3.1}$$

where $V(t) \equiv \langle V(\theta,t)\rangle_\theta$ is the excitatory output averaged over all orientations, with $\langle\cdots\rangle_\theta = \int_0^\pi d\theta/\pi$. It is also useful to define the average value of the excitatory potential, $v(t) \equiv \langle v(\theta,t)\rangle_\theta$, and the average value of the external stimulus, $I \equiv \langle I(\theta)\rangle_\theta$.

The potential of each excitatory neuron depends explicitly on its orientation preference only through the external stimulus (equation 3.1). Hence, neglecting transients, it can be expressed by

$$v(\theta,t) = v(t) + I(\theta) - I \tag{3.2}$$

The mean output of the excitatory neurons can then be related to the mean excitatory potential by an instantaneous gain function, that is, $V(t) = G[v(t)]$, where

$$G(v) \equiv \langle g(v + I(\theta) - I)\rangle_\theta \tag{3.3}$$

The equations for the average potentials $v(t)$ and $u(t)$ are found by averaging the equations for the cluster over all orientations (equation 3.1):

$$\begin{aligned} \dot{v}(t) &= -v(t) + J_E G(v) + J_I g(u) + I \\ \dot{u}(t) &= -u(t) + J'_E G(v) \end{aligned} \tag{3.4}$$

The dynamics of an isolated cluster is particularly simple in that all of the excitatory neurons have the same input except for a stationary, external contribution that depends on the orientation preference of the neuron (equation 3.2).

Figure 2a shows the state diagram for the output (equation 3.4) in terms of the values of two parameters, the inhibitory synaptic strength J_I and the average external input I, with all other parameters held constant. The value of the neuronal gain parameter β was chosen to be large. In this limit the stable fixed points, whenever they exist, correspond to either

an "OFF" state or an "ON" state. In the "ON" state *all* of the neurons are firing near their saturation level, that is, $v(\theta, t) = v(\theta) \approx 1$, while in the "OFF" state all of the neurons are essentially quiescent. In the region marked "ON + OFF", the network is stable in either state and the behavior depends on the initial condition. In the "OSC" region, almost all initial conditions will lead to oscillatory outputs, while in the "OSC + ON" region, depending on the initial condition, the outputs will either oscillate or remain constantly active.

An example of the output for an oscillatory state is displayed in Figure 2b. All the neurons oscillate with the same frequency, as implied by equation 3.2, but their average firing rates differ. The excitatory neurons with the greatest external input, that is, $\theta \approx \theta_0$, are the first to fire within a cycle. They are followed by the neurons with weaker external input and the inhibitory neuron. The output of the inhibitory neuron gradually quenches the activity in the network until the external input again charges the excitatory neurons to a potential above their threshold level. Then the cycle begins anew.

An important characteristic of a cluster is the tuning curve, that is, the average firing rate of an excitatory neuron, $V(\theta) \equiv \langle V(\theta, t) \rangle_t$, where $\langle \cdots \rangle_t$ denotes an average over time. This quantity is a function of the difference between θ and the orientation of the stimulus, θ_0. An evaluation of $V(\theta)$ for different values of θ_0 yields the tuning curve shown in Figure 2c. For the particular form of the input we chose, the activity of the neuron is essentially zero for $|\theta - \theta_0| > 40°$.

4 Phase Description of Interacting Clusters

4.1 Phase Equations. The dynamics of a network of interacting clusters can be greatly simplified in the limit that the intercluster coupling strength is small, that is, $\epsilon \ll 1$. First, equation 2.1 can be reduced to a set of closed mean-field equations that involve only the *average* excitatory and inhibitory potentials of the clusters, $v_R(t)$ and $u_R(t)$, respectively, and the average input, I (Appendix A). Second, it can be shown (Winfree 1980; Kuramoto 1984) that the average potentials are of the form

$$\begin{aligned} v_R(t) &= v_R^o[\omega t + \psi_R(t)] + O(\varepsilon) \\ u_R(t) &= u_R^o[\omega t + \psi_R(t)] + O(\varepsilon) \end{aligned} \tag{4.1}$$

where $v_R^o(t)$ and $u_R^o(t)$ are the limit cycle solutions for the unperturbed cluster (equation 3.4), ω is the frequency of the neuronal oscillation, and $\psi_R(t)$ is the phase of the oscillation. In the absence of intercluster couplings, each of the $\psi_R(t)$ are arbitrary constants whose values lies between O and 2π. The presence of a small coupling between the clusters induces temporal variations in the phases that are slow compared with the period

of the unperturbed limit cycle, that is, $\dot{\psi}_R(t) \approx O(\epsilon)$. These variations are described by phase equations of the form

$$\varepsilon^{-1}\dot{\psi}_R(t) = -\sum_{R' \neq R} K(R - R')\Gamma_{RR'}(\psi_R - \psi_{R'}) + \eta_R(t) \qquad (2)$$

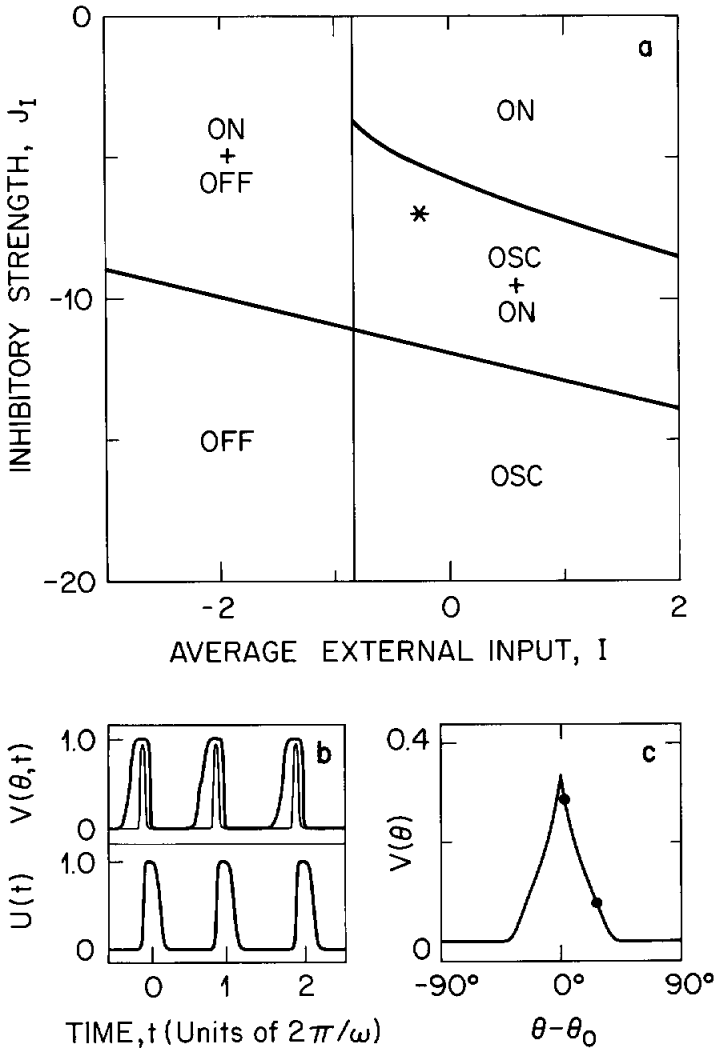

where $\Gamma_{RR'}(\psi_R - \psi_{R'})$ represents the pair-wise interaction between the phases $\psi_R(t)$ and $\psi_{R'}(t)$, and $\eta_R(t)$ is a gaussian noise that originates from $\xi_R(t)$ and has a variance with an amplitude of $\tilde{T} \approx T$ (see equation 2.4). The dynamics of the phases depends on the intercluster interaction $\Gamma_{RR'}(\psi_R - \psi_{R'})$.

4.2 The Form of the Interaction between Phases. The interaction $\Gamma_{RR'}(\psi_R - \psi_{R'})$ is a periodic function, with period $2\pi/\omega$. Its form depends on the structures of the unperturbed limit cycles of the Rth and R'th clusters. In our model the clusters are identical except for the orientation of their respective stimuli, $\theta_0(R)$ and $\theta_0(R')$. Thus $\Gamma_{RR'}(\psi_R - \psi_{R'})$ depends on R and R' only through the relative orientation $\Delta\theta_0 \equiv |\theta_0(R) - \theta_0(R')|$. This implies that $\Gamma_{RR'}(\psi_R - \psi_{R'}) = \Gamma(\Delta\psi; \Delta\theta_0)$, where $\Delta\psi \equiv \psi_R - \psi_{R'}$.

We have derived numerically, using the method of Kuramoto (1984), the form of $\Gamma(\Delta\psi; \Delta\theta_0)$ from the mean-field equations for the potentials of the clusters (Appendix A). The results are shown in Figure 3a. Several features of $\Gamma(\Delta\psi; \Delta\theta_0)$ are apparent. First, it vanishes for $\Delta\theta_0 > \theta_c$, where

---

Figure 2: *Facing page.* Aspects of the dynamics of a single cluster. (a) A state diagram of the output of the network. The fixed parameters for the network were $J_E = 15$, $J_{E'} = 12$, $x_0 = 1.1$, $\beta = 3$, $T = 0$, and $\varepsilon = 0$ and the stimulus profile was $I(\theta - \theta_0) \equiv I_l + (I_h - I_l)|\theta - \theta_0|/(\pi/2)$ with $I_h - I_l = 3.5$. The value of J_I and the average input $I = 1/2(I_h + I_l)$ were varied. The boundaries of existence of the different states were determined from numerical simulations of equations 3.3 and 3.4. However, since β is large, the boundaries for the "ON" or "OFF" states are approximately straight lines that can be determined from equation 3.1 by a consistency analysis. In an "OFF" state the maximum potential of the excitatory neurons must be less than x_0. Since $v(\theta) = I(\theta)$ in this state, we require maximum$[I(\theta)] < x_0$, which yields the vertical line. In the "ON" state the minimal potential has to be larger than x_0. In this state $v(\theta) = J_E + J_I + I(\theta)$ $\dot{v} = 0$ and $V = U = 1$, which leads to $J_E + J_I +$ minimum$[I(\theta)] \simeq x_0$ and yields the oblique line. The asterisk corresponds to the values $J_I = -7$ and $I = -0.25$ used in the simulations for b–c. (b) The average firing rate of two excitatory neurons (upper panel) and the inhibitory neuron (lower panel) found from a simulation of the equations (equation 2.1) for a network with 60 neurons using the above parameters, except that we include noise amplitude $T = 0.0006$ (equation 2.4). We chose the initial conditions such that the neurons did not get stuck in an "ON" state. The heavy line for the excitatory neurons refers to one with an orientation preference $\theta - \theta_0 = 3°$ while the thin line refers to one with $\theta - \theta_0 = 27°$. The period is $2\pi/\omega = 3.4$. (c) The tuning curve, or time-averaged output of an excitatory neuron as a function of its orientation preference relative to the orientation of the stimulus. The average was calculated from simulations of the network with an averaging time of approximately 20 periods. The dots indicate the orientation preferences of the excitatory neurons featured in b.

θ_c is the full extent of the tuning curve ($\theta_c \approx 80°$ in Figure 2c). This can be understood by recalling that only neurons with the same orientation preference are connected by the intercluster couplings. Thus for $\Delta\theta_0 > \theta_c$ there are no pairs of *active* neurons that have the same orientation preference and the effective interaction between the clusters must vanish. Second, $\Gamma(\Delta\psi; \Delta\theta_0)$ is not monotonic in $\Delta\theta_0$. Third, $\Gamma(\Delta\psi; \Delta\theta_0)$ is not an odd function of $\Delta\psi$. This implies that the phase equations *cannot* be described in terms of a potential, that is, the interaction terms in equation 4.2 cannot be written in the form $\partial W/\partial\psi_R$. This has important consequences on the dynamics of a network with many stimulated clusters (Discussion).

The form of $\Gamma(\Delta\psi; \Delta\theta_0)$ indicates that it contains significant contributions from high harmonics in $\Delta\psi$ (Figure 3a). We find that a good approximation is

$$\Gamma(\Delta\psi; \Delta\theta_0) \approx \Gamma_0 + \Gamma_1 \sin(\Delta\psi + \alpha_1) + \Gamma_2 \sin(2\Delta\psi + \alpha_2) \tag{4.3}$$

as illustrated for $\Delta\theta_0 = 15°$ in Figure 3a. The zeroth harmonic, with amplitude Γ_0, represents the shift in the period of the oscillations and is presently irrelevant. The amplitudes Γ_1 and Γ_2 decrease monotonically with $\Delta\theta_0$ and are zero for $\Delta\theta_0 > \theta_c$ (Fig. 3b). An unexpected result is the presence of large phase parameters, α_1 and α_2. They are nonzero even at $\Delta\theta_0 = 0°$ and increase with increasing values of $\Delta\theta_0$. The nonzero value of the phase parameters appears to originate from the inhibitory feedback within each cluster. Specifically, the long-range excitatory synaptic input to weakly active neurons, that is, those stimulated away from their preferred orientation, increases the activity of these neurons and, in turn, increases the activity of the inhibitory neuron. This indirect activation of the inhibitory neuron contributes an "inhibitory" component to the interaction between the clusters. For sufficiently large values of $\Delta\theta_0$, all connections between a pair of clusters involve weakly active neurons and the inhibitory contributions dominate $\Gamma(\Delta\psi; \Delta\theta_0)$.

4.3 Dynamics of Two Interacting Clusters. We consider in detail the case of only two interacting clusters, for which one can subtract the equation of $\dot{\psi}_{R'}(t)$ from that for $\dot{\psi}_R(t)$ (equation 4.2) to obtain an equation for the phase difference $\Delta\psi(t)$:

$$\Delta\dot{\psi}(t) = -\tilde{\Gamma}(\Delta\psi; \Delta\theta_0) + \tilde{\eta}(t) \tag{4.4}$$

where $\tilde{\Gamma}(\Delta\psi; \Delta\theta_0) \equiv \Gamma(\Delta\psi; \Delta\theta_0) - \Gamma(-\Delta\psi; \Delta\theta_0)$ and $\tilde{\eta}(t) = \sqrt{2}\eta(t)$. In the absence of noise, the steady-state solution of equation 4.4 is a fixed point and the phase difference between the two clusters will approach a constant, $\Delta\psi_o$. The value of $\Delta\psi_o$ is determined from the constraints $\tilde{\Gamma}(\Delta\psi_o; \Delta\theta_0) = 0$ and $\partial\tilde{\Gamma}(\Delta\psi_o; \Delta\theta_0)/\partial(\Delta\psi) > 0$. Note that $\tilde{\Gamma}(\Delta\psi; \Delta\theta_0)$

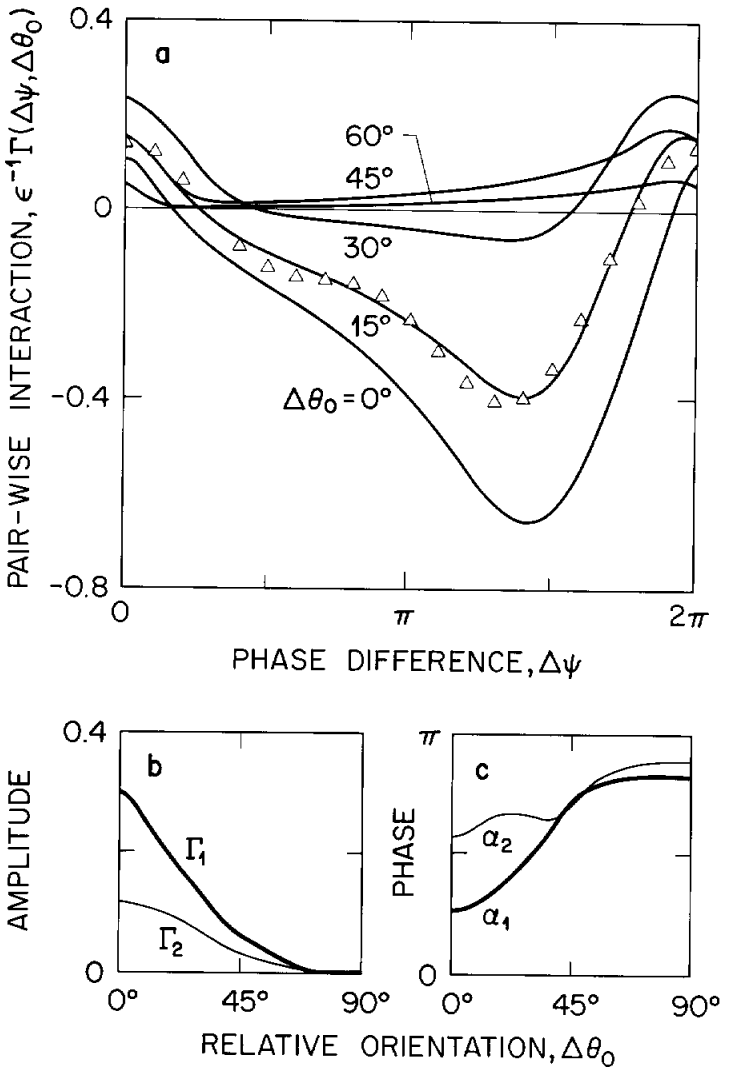

Figure 3: The interaction in a network of weakly coupled clusters. (a) The form of the effective long-range interaction between pairs of phase variables as a function of the relative difference in their phase (equation 4.2). Each curve corresponds to a different value of $\Delta\theta_0$, the relative orientation of the stimuli. Note that the curves for $\Delta\theta_0 = 75°$ and $90°$ are essentially flat. The open symbols correspond to the form of $\tilde{\Gamma}(\Delta\psi; 15°)$ given by its first three harmonics (equation 4.3). (b) The dependence of the amplitude and phase (radians) parameters for the first two harmonic of the interaction (a) on θ_0 (equation 4.3).

is an odd function of $\Delta\psi$. Thus $\Delta\psi = 0$ and π are always zeros of $\tilde{\Gamma}(\Delta\psi; \Delta\theta_0)$, although they are not necessarily stable solutions. Further, the fixed points form degenerate pairs, $\pm\Delta\psi_o$, that, except for the cases $\Delta\psi_o = 0$ or π, correspond to two different states.

The shape of $\tilde{\Gamma}(\Delta\psi; \Delta\theta_0)$ is shown in Figure 4a for several values of $\Delta\theta_0$. For small values the stable state is $\Delta\psi_o = 0$. As $\Delta\theta_0$ is increased (beyond 6° for our parameters) the fixed point moves to a nonzero, intermediate value of $\Delta\psi_o$. As $\Delta\theta_0$ is further increased (beyond 36°) the stable fixed point becomes $\Delta\psi_o = \pi$ and remains so until the force vanishes (beyond 80°). This behavior can be qualitatively understood by approximating $\tilde{\Gamma}(\Delta\psi; \Delta\theta_0)$ in terms of its first two harmonics (equation 4.3), that is, $\tilde{\Gamma}(\Delta\psi; \Delta\theta_0) \approx 2\Gamma_1 \cos\alpha_1 \sin(\Delta\psi) + 2\Gamma_2 \cos\alpha_2 \sin(2\Delta\psi)$. When the first harmonic dominates the interaction, as occurs when the value of α_1 is substantially smaller than $\pi/2$ and Γ_1 is substantially larger than Γ_2, the phase difference is zero. This situation corresponds to small values of $\Delta\theta_0$ (Fig. 3b and c). Similarly, a value of α_1 near π leads to a phase difference of π, as occurs for large values of $\Delta\theta_0$. When the value of α_1 is near $\pi/2$, corresponding to intermediate values of $\Delta\theta_0$, the contribution from the first harmonic is of the same magnitude of that from the second. This gives rise to the pronounced anharmonic shape of $\tilde{\Gamma}(\Delta\psi; \Delta\theta)$ (Fig. 4a) and to an intermediate phase shift $\Delta\psi_o \approx \cos^{-1}(-\Gamma_1 \cos\alpha_1 / 2\Gamma_2 \cos\alpha_2)$.

In the presence of noise, $\tilde{\eta}(t)$ in equation 4.4, the phase difference $\Delta\psi$ fluctuates in time rather than approach a fixed value. The average phase coherence between the two clusters can be expressed by the intercluster correlation function

$$C_{RR'}(\tau) \equiv \frac{\langle \delta V_R(t) \delta V_{R'}(t+\tau) \rangle_t}{\sqrt{\langle \delta V_R^2(t) \rangle_t \langle \delta V_{R'}^2(t) \rangle_t}} \tag{4.5}$$

with $\delta V_R(t) \equiv V_R(t) - \langle V_R(t) \rangle_t$ and, as before, $\langle \cdots \rangle_t$ denotes an average over time. The correlation function can be calculated from the unperturbed limit cycle of a single cluster and the phase dynamics (Appendix B). Since the clusters are identical, and the interaction between them is symmetric, an extremum will always occur at $\tau = 0$.

The correlation function for several values of $\Delta\theta_0$ are shown in Figure 4b–d. When both stimuli are aligned, that is, $\Delta\theta_0 = 0°$, the

Figure 4: *Facing page.* Aspects of the dynamics in a network with two clusters. (a) The force that acts on the difference between two clusters as a function of their relative phase difference (equation 4.2). Each curve corresponds to a different value of $\Delta\theta_0$; those for $\Delta\theta_0 = 75°$ and 90° are essentially flat. (b–d) The intercluster correlation function of the phase difference between two clusters as a function of time and different values of $\Delta\theta_0$ (equations 4.5 and B.4). The thin line refers to a low level of noise, $1/T = 33$, and the thick line refers to an intermediate level, $1/T = 3.3$. The network was equilibrated for approximately 150 periods and the correlation functions were averaged over an additional 150 periods.

correlation has a prominent peak at $\tau = 0$ (Fig. 4b). As the relative angle between the stimuli is increased, $C_{RR'}(\tau)$ develops a double peak that reflects the fluctuation of the network between two stable intermediate phase shifts. The presence of these phase-shifts also causes a minimum to occur at $\tau = 0$. These features are seen at $\Delta\theta_0 = 30°$, for which

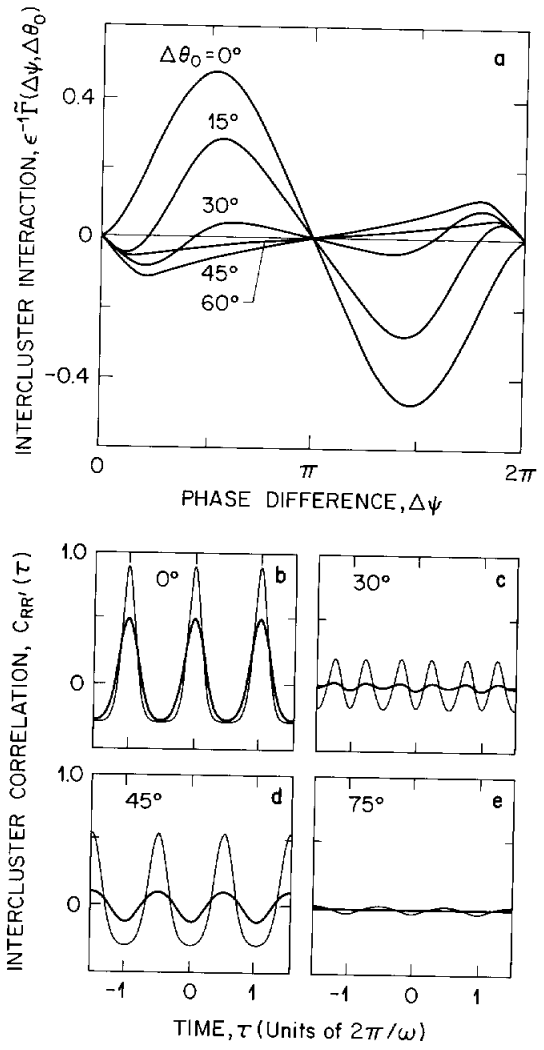

$\Delta\psi_o \simeq \pm 1.3$ (Fig. 4c). Note that, in practice, the intermediate phase shift may show up as a single peak at either a positive or a negative value of τ if the activity of the network is averaged for only a short time. Lastly, the peak amplitude of $C_{RR'}(\tau)$ is not a monotonic function of $\Delta\theta_0$ (cf. Fig. 4b–e). Further, while noise suppresses the amplitude of $C_{RR'}(\tau)$ for any value of $\Delta\theta_0$, the suppression is greatest for intermediate values (cf. thick versus thin line in Fig. 4c). These features reflect the nonmonotonic behavior of $\tilde{\Gamma}(\Delta\psi; \Delta\theta_0)$ with respect to $\Delta\theta_0$ (Fig. 3a).

We calculated the equal-time correlation coefficient, $C_{RR'}(0)$, as a function of the relative orientation of two stimuli, $\Delta\theta_0$, and for two levels of noise, $\tilde{T}$ (Fig. 5). The value of the coefficient rapidly decreases as a function of the relative orientation for either case. Beyond approximately the full-width at half-maximum of the tuning curve, 22° for our parameters (Fig. 2c), the coefficient becomes negative as a consequence of the substantial phase-shifts that occur for large values of $\Delta\theta_0$. However, as the magnitude of the interaction is reduced for these angles, the corresponding magnitude of the coefficients is also significantly reduced, particularly at high levels of noise.

5 Discussion

Our main result is that a weak, fixed synaptic coupling between clusters of neurons can generate an effective interaction between the phases of their oscillatory response that depends strongly on the distribution of activity within each cluster. Thus the interaction is sensitive to the dissimilarity of the external inputs that stimulate the clusters. This result implies that stimulus-dependent synchronizing connections, postulated ad hoc in a previous network model of phase oscillators (Sompolinsky *et al.* 1990, 1991), can originate from neuronal dynamics without the need to invoke mechanisms of fast synaptic modification. This conclusion is consistent with the results of Konig and Schillen (1991), who simulated a network with time delayed connections and with the initial reports of Sporns *et al.* (1989).

Our phase description is strictly valid only in the limit of weak intercluster coupling. In practice, the results of numerical calculations of the full equations for the model (equation 2.1) indicate that the phase model qualitatively describes the dynamics of the clusters even when the synaptic input a neuron receives via intercluster connections is about 5% of its total input ($\varepsilon = 0.02 J_E$; data not shown). The time it takes to synchronize the output of two clusters from an initial, unsynchronized state is relatively short, about three cycles for this strength of interaction (insert to Fig. 5).

In contrast to the ad hoc assumption in a previous work (Sompolinsky *et al.* 1990, 1991), the present analysis shows that dissimilarity in the external stimuli for each of the two clusters not only reduces the amplitude

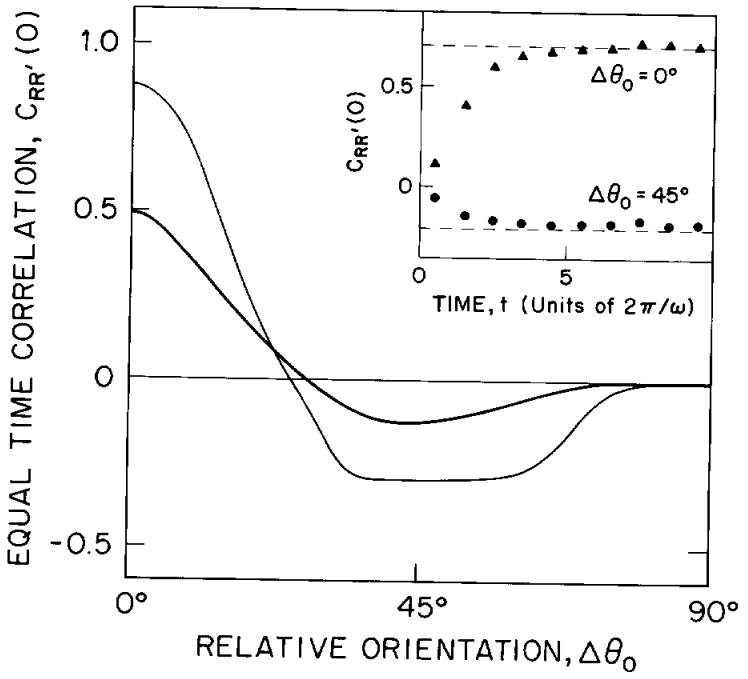

Figure 5: The equal-time intercluster correlation coefficient for the phases difference between two clusters as a function of $\Delta\theta_0$ (equations 4.5 and B.4 with $\tau = 0$). This coefficient is a measure of the discrimination capability of the network. The thin line is for $1/T = 33$, while the thick line is for $1/T = 3.3$. The inset shows the amplitude of the coefficient during consecutive periods following the presentation of stimuli. Equations 2.1–2.4 were simulated numerically with the parameters used in the phase model (legend to Fig. 2a), $1/T = 3.3$ and $\varepsilon = 0.02J_E$. Each datum reflects an average over 64 random initial conditions of the network.

of their effective interaction but also induces a tendency to form phase-shifts. When only two clusters are stimulated, the phase-shifts appear in the intercluster correlation function (equation 4.5; Fig. 4c–e). Large differences in orientation between the two stimuli result in a phase shift of π (Fig. 4d and e). The phase shifts are less than π for intermediate differences in orientation and disappear for small differences.

Our results with regard to the occurrence of phase shifts are in apparent contradiction to those of Schuster and Wagner (1990a). These authors studied the phase interaction between weakly coupled clusters of neu-

rons and claim that significant phase shifts do not occur. In contrast to the present work, the clusters in the model of Schuster and Wagner (1990a) had uniform external inputs and, further, their analysis was restricted to parameters near a Hopf bifurcation where the nonlinearities in the dynamics are weak. Our results are consistent with the simulations of Schillen and Konig (1991), where phase-shifts in the correlation between the output of two clusters are evident (see their Fig. 4).

There is currently little experimental evidence for phase shifts among the oscillatory responses of neurons in visual cortex [but note Fig. 1g in Engel *et al.* (1991b)]. This is in apparent disagreement with the predictions of our model. One possibility is that the limit of weak, long-range coupling is inappropriate. Yet this limit is suggested from the experimental evidence on stimulus dependent synchronization across visual cortex (Eckhorn *et al.* 1988; Gray *et al.* 1989). In brief, stimuli outside the receptive field of a neuron may affect the cross-correlogram between it and other cells but these stimuli do not significantly perturb the magnitude or form of its autocorrelogram. This suggests that the effective interaction between distant neurons affects only their timing and not their rate of firing. A second possibility is that phase-shifts are particular to our choice of local architecture (Fig. 1). The numerical studies of Konig and Schillen (1991) make use of an architecture with solely excitatory connections plus synaptic delays, rather than inhibitory feedback. As mentioned above, the output of different clusters in their model exhibits phase-shifts. Further, Hansel *et al.* (1992) recently derived the form of the phase interaction between two Hodgkin–Huxley neurons. They show that shifts occur for a range of inputs with neurons coupled either by synapses or electrotonic junctions. Thus a body of evidence suggests that phase-shifts are a generic feature of the interaction between weakly coupled neuronal oscillators.

There are a number of experimental issues that relate to the observation of phase shifts. The fully averaged cross-correlogram is symmetric in the presence of shifts. However, the cross-correlogram is likely to appear asymmetric when the averaging is incomplete so that only one of the two possible phases, $\Delta\psi = \pm\Delta\psi_0$ (Fig. 4a), dominates the interaction. Thus asymmetric cross-correlograms, traditionally interpreted as the signature of monosynaptic connections (Perkel *et al.* 1967), may in some cases reflect phase-shifted correlograms that have been averaged for too short a time. A second issue is that fluctuations in cortical activity may make shifts difficult to detect. The amplitude of the phase-shifted correlograms is expected to be reduced compared with correlograms without phase shifts (cf. Fig. 4a and c–e). This may significantly lower the signal-to-noise ratio of shifted cross-correlograms. However, even in the presence of noise stimulus-dependent phase-shifts should lead to a change in the shape of the cross-correlogram that depends on the form of the stimuli. Indeed, cross-correlograms whose shape depends on the orientation of the stimulus have been observed (Ts'o *et al.* 1986). Lastly, both noise and variations

in the intrinsic frequency of the oscillation will broaden the phase-shifted peaks in the correlogram. This may cause a shifted correlogram to appear as one with a relatively broad central peak. Such correlograms have been reported in recent studies (Nelson *et al.* 1992), although it is unclear if they result from the mechanism we propose. We suggest that the existence of phase shifts in the oscillatory part of neuronal responses to dissimilar stimuli deserves further experimental scrutiny.

The presence of phase parameters can lead to dramatic changes to the phase dynamics (equation 4.2) when more than two clusters of neurons are stimulated. While the detailed behavior depends on the form of the intercluster interaction, $\Gamma_{RR'}(\psi_R - \psi_{R'})$, qualitative aspects of the behavior may be accounted for by the simplified model

$$\begin{aligned} \varepsilon^{-1}\dot{\psi}_R(t) &= -\sum_{R' \neq R} K(R - R')\, J(\Delta\theta_0) \sin\left(\psi_R - \psi_{R'} + \alpha(\Delta\theta_0)\right) \\ &\quad + \eta_R(t) \end{aligned} \tag{5.1}$$

Here $\Delta\theta_0 = \theta_0(R) - \theta_0(R')$ is the relative orientation of the particular two of stimuli that act on a pair of clusters. The interaction parameter, $J(\Delta\theta_0)$, measures the average overlap of the activities in a pair of clusters. It decreases monotonically with increasing values of $\Delta\theta_0$ and vanishes for $\Delta\theta_0 > \theta_c$, where θ_c is the full width of the tuning curve. Conversely, the phase parameter $\alpha(\Delta\theta_0)$ increases monotonically with $\Delta\theta_0$. As before, $K(R - R')$ specifies the spatial extent of the long-range connections (equation 2.1), and $\eta_R(t)$ is a gaussian noise (equation 4.2). The above model explicitly expresses the dependence of the amplitudes and phases of the interaction between the clusters on relative phases of each cluster on the spatial distribution of gradients in the orientation of the stimuli.

When the phase parameters $\alpha(\Delta\theta_0)$ are zero, as assumed in a previous work (Sompolinsky *et al.* 1990, 1991), the network is unfrustrated. In the absence of noise the stimulated clusters will synchronize with zero phase shifts. In contrast, nonzero values of $\alpha(\Delta\theta_0)$ may induce substantial frustration into the network and lead to a stable state with a complicated pattern of phase shifts. Further, the dynamics of the network is not governed by an energy function and thus the phases may not converge to fixed values. In cases where the values of phase parameters are large, such as when the stimulus contains sufficiently large spatial gradients, it is likely that the phases of each cluster, $\Psi_R(t)$, will fluctuate chaotically in time.

The phase model proposed here (equation 5.1) is likely to have validity beyond the specific architecture and dynamics of the circuit in the present work (Fig. 1). In fact, the simulation results of other circuits proposed for the 40 Hz oscillations in visual cortex (Sporns *et al.* 1991; Buhmann and von der Malsburg 1991; Konig and Schillen 1991; Wilson and Bower 1991) can be interpreted by this phase model. Thus, the model may provide a useful framework to probe the nature of spatiotemporal patterns of neuronal responses and their role in sensory processing.

Appendix A

Here we sketch our derivation of the phase description from the full dynamics of the network. The equations for the dynamics of the full network (equation 2.1) are first reduced to a set of equations that involve only the potentials $v_R(t)$, and $u_R(t)$, the input I, and the noise $\xi_R(t)$ within the clusters. This is accomplished by averaging equation 2.1 over all orientations θ, so that

$$\begin{aligned} \dot{v}_R(t) &= -v_R(t) + J_E V_R(t) + J_I U_R(t) + I + \xi_R(t) \\ &\quad + \varepsilon \sum_{R' \neq R} K(R - R') V_{R'}(t) \\ \dot{u}_R(t) &= -u_R(t) + J'_E V_R(t) \end{aligned} \tag{A.1}$$

To close these equations, one must obtain a relationship between the average output V_R and the average potentials, $v_R(t)$ and $u_R(t)$. Subtracting equation 2.1 from equation A.1 and expanding all terms to first order in ε yields

$$V_R(t) = G[v_R(t)] + \varepsilon \sum_{R' \neq R} \Upsilon_{RR'}(v_R, v_{R'}; t) \tag{A.2}$$

where

$$\begin{aligned} \Upsilon_{RR'}(v_R, v_{R'}; t) &\equiv K(R - R') \int_{-\infty}^{t} d\tau e^{-(t-\tau)} \\ &\quad \langle g'(u_R(t) + I_R(\theta) - I) \delta g(v_{R'}(\tau) + I_{R'}(\theta) - I) \rangle_\theta \end{aligned} \tag{A.3}$$

with $g'(x) \equiv dg/dx$ and $\delta g(x) \equiv g(x) - \langle g(x) \rangle_\theta$. Substitution of equations A.2 and A.3 into equation A.1 gives

$$\begin{aligned} \dot{v}_R(t) &= -v_R(t) + J_E G[v_R(t)] + J_I g[u_R(t)] + I + \xi_R(t) \\ &\quad + \varepsilon \sum_{R' \neq R} \tilde{\Upsilon}_{RR'}(v_R, v_{R'}; t) \\ \dot{u}_R(t) &= -u_R(t) + J'_E G[v_R(t)] + \varepsilon \sum_{R' \neq R} \Upsilon_{RR'}(v_R, v_{R'}; t) \end{aligned} \tag{A.4}$$

where

$$\tilde{\Upsilon}_{RR'}(v_R, v_{R'}; t) = K(R - R')G[v_R(t)] + \Upsilon_{RR'}(v_R, v_{R'}; t) \tag{A.5}$$

and $G(x)$ is defined by equation 3.3.

The intercluster interaction term in equation A.4 is nonlocal in time. However, for small values of ε the potentials can be approximated by $v_R(t) = v_R^o[\omega t + \psi_R(t)]$ and $v_{R'}(t) = v_{R'}^o[\omega t + \psi_{R'}(t)]$, where we have used equation 4.4 and the fact that the phases vary slowly on the time scale of the period for the oscillations, $2\pi/\omega^{-1}$. Substituting this form into equation A.4 results in equations that are now local in time. These equations represent a system of weakly coupled, two-dimensional limit cycles. By an appropriate average over the fast variables, they are further reduced to a set of equations (equation 4.2) that involves only the slow, phase variables, $\psi_R(t)$ (Fig. 3). For details of this reduction, see Kuramoto (1984).

Appendix B

Here we sketch our calculations of the intercluster correlation function (equation 4.5) in terms of the phase dynamics. The correlation can be expressed as

$$C_{RR'} = \frac{\langle \delta V_R^o[\omega t + \psi_R(t)] \delta V_{R'}^o(\omega t + \omega\tau + \psi_{R'}[t + \tau)]\rangle_t}{\langle \{\delta V_R^o[\omega t + \psi_R(t)]\}^2\rangle_t} \tag{B.1}$$

where $\langle \cdots \rangle_t$ denotes averaging over time *and* over the noise in the phase equations (equation 4.2) and $\delta V_R^o[\omega t + \psi_R(t)] \equiv V_R^o[\omega t + \psi_R(t)] - \langle V_R(t)\rangle_t$ where $V_R^o[\omega t + \psi_R(t)] \approx G\{v_R^o[\omega t + \psi_R(t)]\}$ is the solution of the equations for the unperturbed cycle (equations 2.2, 3.3, and 3.4). If we restrict ourselves to values of τ that are on the order of ω^{-1}, we can make the approximation $\psi_{R'}(t + \tau) \approx \psi_{R'}(t)$. In this limit $C_{RR'}(\tau)$ depends only on fluctuations in the phase difference $\Delta\psi(t) = \psi_{R'}(t) - \psi_R(t)$.

For the case when only two clusters are stimulated, the form of equation 4.4 implies that the equilibrium distribution of the phase difference, a stochastic variable, is of a Gibbs' form, that is,

$$D(\Delta\psi) \propto e^{-W(\Delta\psi)/2\tilde{\Gamma}} \tag{B.2}$$

where the potential $W(\Delta\psi)$ is given in terms of the interaction $\tilde{\Gamma}(\Delta\psi; \Delta\theta_0)$ (equation 4.4) by

$$W(\Delta\psi) = \int_0^{\Delta\psi} d\psi \tilde{\Gamma}(\psi; \Delta\theta_0) \tag{B.3}$$

We thus arrive at

$$C_{RR'}(\tau) = \frac{\int_0^{2\pi}(d\psi/2\pi)D(\psi)\int_0^{2\pi\omega^{-1}}(\omega dt/2\pi)\delta V_R^o(\omega t)\delta V_{R'}^o(\omega t + \omega\tau + \psi)}{\langle[\delta V_R^o(t)]^2\rangle_t} \tag{B.4}$$

Note that this result for $C_{RR'}(\tau)$ is valid only for values $\tau \approx O(\omega^{-1})$.

Acknowledgments

We thank B. Friedman, C. D. Gilbert, D. Hansel, J. A. Hirsch, P. C. Hohenberg, P. Konig, O. Sporns, and D. Y. Ts'o for useful discussions. D. K. and H. S. thank the Aspen Center for Physics for its hospitality. This work was supported, in part, by the Fund for Basic Research administered by the Israeli Academy of Arts and Sciences and by the U.S.–Israel Binational Science Foundation.

References

Aertsen, A. M. H. J., Gerstein, G. L., Habib, M. K., and Palm, G. 1989. Dynamics of neuronal firing correlation: Modulation of effective connectivity. *J. Neurophys.* **61**, 900–917.

Amari, S.-I. 1972. Learning patterns and patterns of sequences by self-organizing nets of threshold elements. *IEEE Trans. Comp.* **21**, 1197–1206.

Bouyer, J. J., Montaron, M. F., and Rougeul, A. 1981. Fast fronto-parietal rhythms during combined focused attentive behaviour and immobility in cat: Cortical and thalamic localization. *Electroenceph. Clim.* **51**, 244–252.

Buhmann, J., and von der Malsburg, Ch. 1991. Sensory segmentation by neural oscillators. In *Proceedings of the International Conference on Neural Networks*, pp. 603–607, Vol. II.

Douglas, R. J., and Martin, K. A. C. 1990. Neocortex. In *Synaptic Organization of the Brain*, 3rd ed., G. M. Shepherd, ed., pp. 356–438. Oxford University Press, New York.

Eckhorn, R., Bauer, R., Jordan, W., Brosch, M., Kruse, W., Munk, M., and Reiboeck, R. J. 1988. Coherent oscillations: A mechanism of feature linking in the visual cortex? Multiple electrode and correlation analysis in the cat. *Biol. Cybern.* **60**, 121–130.

Engel, A. K., Konig, P., Kreiter, A. K., and Singer, W. 1991a. Interhemispheric synchronization of oscillatory neuronal responses in cat visual cortex. *Science* **252**, 1177–1180.

Engel, A. K., Kreiter, A. K., Konig, P., and Singer, W. 1991b. Synchronization of oscillatory neuronal responses between striate and extrastriate visual cortical areas of the cat. *Proc. Natl. Acad. Sci. U.S.A.* **88**, 6048–6052.

Freeman, W., and van Dijk, B. W. 1987. Spatial patterns of visual cortical fast EEG during conditioned reflex in a rhesus monkey. *Brain Res.* **422**, 267–276.

Gilbert, C. D., and Wiesel, T. N. 1989. Columnar specificity of intrinsic horizontal and corticocortical connections in cat visual cortex. *J. Neurosci.* **9**, 2432–2442.

Gray, C. M., Konig, P., Engel, A. K., and Singer, W. 1989. Oscillatory responses in cat visual cortex exhibit intercolumnar synchronization which reflects global stimulus properties. *Nature (London)* **338**, 334–337.

Hansel, D., Mato, G., and Meunier, C. 1992. Phase dynamics for weakly coupled model neurons. *CNRS preprint.*

Hopfield, J. J. 1984. Neurons with graded response have collective computational properties like those of two-state neurons. *Proc. Natl. Acad. Sci. U.S.A.* **8**, 3088–3092.

Ketchum, K. L., and Haberly, L. B. 1991. Fast oscillations and dispersive propagation in olfactory cortex and other cortical areas: A functional hypothesis. In *Olfaction: A Model System for Computational Neuroscience*, J. L. Davis and H. Eichenbaum, eds., pp. 69–100. MIT Press, Cambridge, MA.

Konig, P., and Schillen, T. B. 1991. Stimulus-dependent assembly formation of oscillatory responses: I. Synchronization. *Neural Comp.* **3**, 155–166.

Kuramoto, Y. 1984. *Chemical Oscillations, Waves, and Turbulence.* Springer-Verlag, New York.

Nelson, J. I., Salin, P. A., Munk, M. H., Arzi, M., and Bullier, J. 1992. Spatial and temporal coherence in cortico-cortical connections: A cross-correlation study in areas 17 and 18 in the cat. *Visual Neurosci.* **9**, 21–37.

Perkel, D. H., Gerstein, G. L., and Moore, G. P. 1967. Neuronal spike trains and stochastic point processes. II. Simultaneous spike trains. *Biophys. J.* **7**, 419–440.

Schillen, T. B., and Konig, P. 1991. Stimulus-dependent assembly formation of oscillatory responses: II. Desynchronization. *Neural Comp.* **3**, 167–178.

Schuster, H. G. 1991. *Nonlinear Dynamics and Neuronal Networks: Proceedings of the 63rd W. E. Heraues Seminar, Friedrichsdorf 1990.* VCH, New York.

Schuster, H. G., and Wagner, P. 1990a. A model for neuronal oscillations in the visual cortex: I. Mean-field theory and the derivation of the phase equations. *Biol. Cybern.* **64**, 77–82.

Schuster, H. G., and Wagner, P. 1990b. A model for neuronal oscillations in the visual cortex: II. Phase description of the feature dependent synchronization. *Biol. Cybern.* **64**, 83–85.

Sompolinsky, H., Golomb, D., and Kleinfeld, D. 1990. Global processing of visual stimuli in a network of coupled oscillators. *Proc. Natl. Acad. Sci. U.S.A.* **87**, 7200–7204.

Sompolinsky, H., Golomb, D., and Kleinfeld, D. 1991. Cooperative dynamics in visual processing. *Phys. Rev. A15* **43**, 6990–7011.

Sporns, O., Gally, J. A., Reeke, G. A., and Edelman, G. M. 1989. Reentrant signaling among simulated neuronal groups leads to coherency in their oscillatory activity. *Proc. Natl. Acad. Sci. U.S.A.* **86**, 7265–7269.

Sporns, O., Tononi, G., and Edelman, G. M. 1991. Modeling perceptual grouping and figure-ground segregation by means of active reentrant connections. *Proc. Natl. Acad. Sci. U.S.A.* **88**, 129–133.

Ts'o, D. Y., Gilbert, C. D., and Wiesel, T. N. 1986. Relationships between horizontal interactions and functional architecture in cat striate cortex as revealed by cross-correlation analysis. *J. Neurosci.* **6**, 1160–1170.

Wilson, W. A., and Bower, J. A. 1991. A computer simulation of oscillatory behavior in primary visual cortex. *Neural Comp.* **3**, 498–509.

Wilson, H. R., and Cowan, J. D. 1972. Excitatory and inhibitory interactions in localized populations of model neurons. *Biophys. J.* **12**, 1–24.

Winfree, A. T. 1980. *The Geometry of Biological Time.* Springer-Verlag, New York.

Received 4 February 1992; accepted 25 January 1993.